

Vectorization of Raster Manga by Deep Reinforcement Learning

Hao Su¹, Jianwei Niu^{1,2,3}, Xuefeng Liu¹, Jiahe Cui¹, Ji Wan¹,

¹State Key Lab of VR Technology and System, School of Computer Science and Engineering, Beihang University

²Industrial Technology Research Institute, School of Information Engineering, Zhengzhou University

³Hangzhou Innovation Institute, Beihang University

{bhsuhao, niujianwei, liu_xuefeng, wanji}@buaa.edu.cn

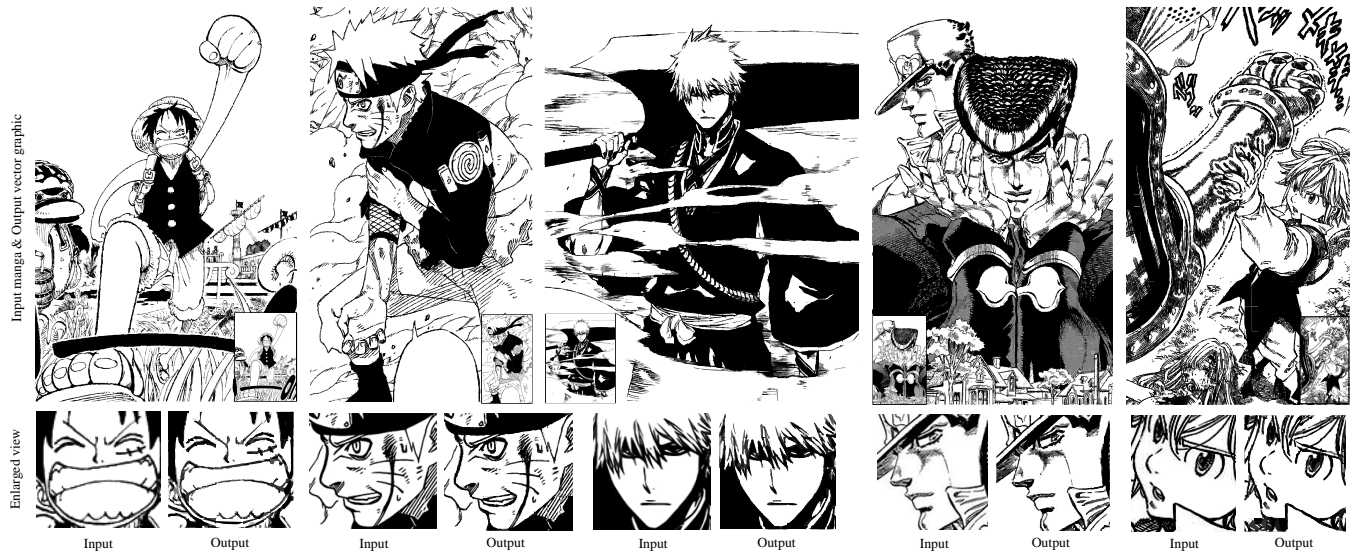


Figure 1: Samples of input raster manga (black bounding-box) and our generated vector graphics. These vector graphics are displayed in PDF format and can be zoomed freely without distortion. Please use digital zoom to better appreciate the quality of the vector graphics. More samples of inputs and outputs are shown in the supplemental material at https://drive.google.com/file/d/1GMFX2QOm2tkBSkG-F_BmDgI5OvnBQop1/view?usp=sharing

Abstract

Manga is a popular Japanese-style comic form that consists of black-and-white stroke lines. Compared with images of real-world scenarios, the simpler textures and fewer color gradients of mangas are the extra natures that can be vectorized. In this paper, we propose *Mang2Vec*, the first approach for vectorizing raster mangas using Deep Reinforcement Learning (DRL). Unlike existing learning-based works of image vectorization, we present a new view that considers an entire manga as a collection of basic primitives "stroke line", and the sequence of strokes lines can be deep decomposed for further vectorization. We train a designed DRL agent to produce the most suitable sequence of stroke lines, which is constrained to follow the visual feature of the target manga. Next, the control parameters of strokes are collected to translated to vector format. To improve our

performances on visual quality and storage size, we further propose an SA reward to generate accurate strokes, and a pruning mechanism to avoid producing error and redundant strokes. Quantitative and qualitative experiments demonstrate that our *Mang2Vec* can produce impressive results and reaches the state-of-the-art level.

1. Introduction

Manga is a popular Japanese-style comic form in the world. Typical mangas are composed of black-and-white stroke lines and represented as raster images on digital multimedia. As shown in Figure 1, compared with images of real-world scenarios, mangas have the extra natures to be vectorized, i.e., having simpler structures and fewer color gradients. The advantages of vectorizing raster manga are four-fold. First, vector graphics are resolution-independent

and readily displayed on digital devices with different resolutions. Second, allowing easily edit the stroke lines and colors. Third, for showing some contents, vector graphics have higher compression ratios for storage than raster images. Fourth, offering convenience for content retrieval, and allowing retrieval for particular shape objects.

Vectorization of raster images has been studied extensively in image processing, graphics, vision, and other areas. Recent representative works for vectorizing images are mainly divided into two categories. The first category of works is based on pre-designed algorithms, which analyzes pixels and calculates parameters to construct vector graphics (e.g., [2, 5, 14, 16, 21, 22, 31]). The other category of works is based on deep learning (DL) (e.g., [4, 6, 8, 18, 23, 27–29]), which trains neural models to produce vector graphics utilizing the features of target raster images. However, the DL-based methods typically vectorize an entire image in one step, and the one-step manner makes the DL model cannot handle too many parameters of vector format accurately. Therefore, these methods only work well in vectorizing targets with simpler structures (e.g., icons, fonts), and get trouble in vectorizing mangas with complex structures¹.

Unlike these works, our proposed Mang2Vec is a vectorization approach based on Deep Reinforcement Learning (DRL). In Mang2Vec, we propose a new view that considers an entire manga as a collection of basic primitives “stroke line”, and the sequence of strokes lines can be deep decomposed for further vectorization. First, start with a blank canvas, we train a DRL agent to produce the most suitable stroke line at each step by the designed rewards. After enough steps, the combination of sequential stroke lines will appear as the input manga. Then, the control parameter of each stroke is collected to be converted to the designed vector format. Since stroke lines can be infinitely added by the DRL model, our approach has better performance on vectorizing mangas with complex textures. To improve our performance on visual quality and storage size, in Mang2Vec, we propose an SA reward to generate accurate strokes, and a pruning mechanism to avoid producing error and redundant strokes. Extensive quantitative and qualitative experiments demonstrate that our Mang2Vec can produce impressive results and has achieved the state-of-the-art level.

To summarize, our main contributions are three-fold:

- We propose Mang2Vec, the first DRL-based approach for vectorizing raster mangas. Mang2Vec presents a new view that considers an entire manga as a sequential of basic primitives “stroke line” that can be deep decomposed for further vectorization.

¹The vectorization accuracies are compared in Figure 5 and Figure 6.

- We propose a new SA reward to improve the accuracy of generated stroke lines in colors and positions, and propose a pruning module to avoid error strokes and reduce the storage size.
- Experiments show that Mang2Vec can produce impressive results, and prove the effectiveness in vectorizing numerous types of mangas with complex structures (e.g., with intensive, sparse, wide, or thin stroke lines).

2. Related Work

Below we summarize the most related works that mainly involve methods of learning-based image vectorization, generative model of vector graphics, and image decomposition.

Learning-based vectorization: the goal of learning-based vectorization methods is to convert a target image to the vector format with high visual similarity. Egiazarian et al. [6] propose a transformer-based architecture for translating technical line drawings to vector parameters. Gao et al. [8] produce parametric curves utilizing the extracted image features and a designed hierarchical recurrent network. Guo et al. [10] sub-divide the lines into partial curves employing a deep network, and reconstruct the topology at junctions. For raster floorplans, Liu et al. [18] first utilize a network to convert an image to junctions, and then address an integer program that obtains the vectorized floorplans as a set of architectural primitives. Reddy et al. [23] propose Im2Vec, a VAE-based method to predict vectorize parameters of input images, and the network can be trained without vector supervision.

Generative model of vector graphic: the motivation of generative vector graphic models is to produce vector graphics by inputting some heuristic information (e.g, incomplete sketches, conditional parameters, random noises), where inputs and outputs do not need accurate correspondences in appearance. SketchRNN [11] propose a method for both unconditional and conditional vector generation. All sketches are translated to pen positions and states, and an LSTM is trained to produce parameters of a density function, where the parameters can be sampled to produce a new sketch. Similar to SketchRNN, Sketchformer [24] presents a framework to encode vector form sketches using the transformer. SVG-VAE [19] is the first generative approach for estimating vector graphics parameters. They fix the weights of pre-trained Variational Auto Encoder (VAE) weights and train a decoder that predicts vector parameters from the latent variable learned on images. DeepSVG [3] shows that the hierarchical networks are useful to reconstruct diverse vector graphics, and do well in interpolation and generation tasks. For font glyphs vectorization, [1, 9] can produce results from partial observations in a low-resolution raster

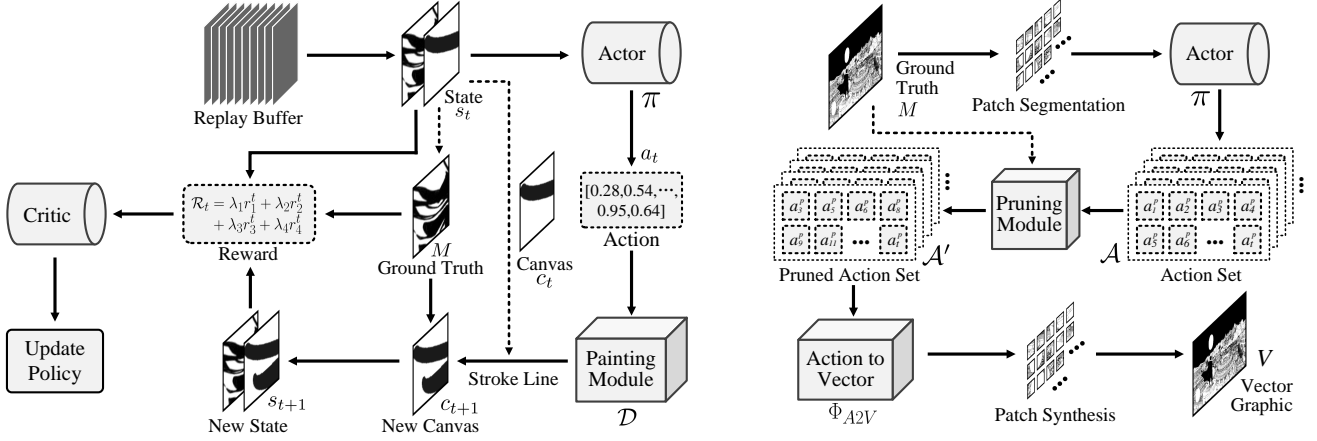


Figure 2: System Pipeline. Given a raster manga image M , our goal is to translate M to a vector graphic \mathcal{V} with accurate visual similarity. **Left:** the learning part Ψ_l that aims to learn a DRL model to produce an action sequence $\mathcal{A} = \Psi_l(M)$, where $\mathcal{A} = \{a_0, a_1, \dots, a_t\}$ can be translated to the stroke line sequence $\mathcal{L} = \{l_0, l_1, \dots, l_t\}$ by a designed drawing model \mathcal{D} , and the combination of all strokes in \mathcal{L} are constrained to compose M visually. **Right:** the vectorization part Ψ_v that aims to convert action sequence \mathcal{A} to vector format \mathcal{V} in a designed manner.

domain. Li et al. [17] present a differentiable rasterizer to edit and produce vector parameters by raster-based target functions and machine learning.

Image decomposition: these methods decompose an image into an assembly of primitives in pixel-wise, which aims to benefit understanding scenes, assisting in classify, reproducing painting processes, and so on. Prior works [7, 13, 20, 32] train DRL drawing agents, and circumvent the requirement of supervision on the painting process by simulating a rendering engine. CSGNet [26] propose a deep model that constructs complex shapes by recursively applying boolean operations on primitives. It designs a neural encoder and recurrent decoder to map shapes to modeling instructions, and trains the network by policy gradient algorithm.

Unlike the above methods, our work combines the merits of image vectorization and image decomposition, and considers an entire manga image as a combination of vector primitives, and generates the sequence of vector primitives that is visually similar to the input manga by the DRL technique.

3. Method

3.1. Overview

Given a raster manga image M , our Mang2Vec is modeled as a function Ψ to generate a vector graphic $\mathcal{V} = \Psi(M)$. For appearance, \mathcal{V} is similar to M accurately. For format, \mathcal{V} is a vector graphic that can be zoomed freely without distortion.

As shown in Figure 2, our Mang2Vec $\Psi = \{\Psi_l, \Psi_v\}$ is composed of two parts, the learning part Ψ_l (Figure 2 left)

and the vectorization part Ψ_v (Figure 2 right). Ψ_l is designed to learn an accurate DRL model for decomposing M to a sequence of primitives parameters, and Ψ_v is designed to further vectorize the primitives parameters. Specifically, in Ψ_l , our goal is to train a DRL model to produce an action sequence $\mathcal{A} = \Psi_l(M)$, where $\mathcal{A} = \{a_0, a_1, \dots, a_t\}$ can be translated to the stroke line sequence $\mathcal{L} = \{l_0, l_1, \dots, l_t\}$ by the designed drawing model \mathcal{D} , represented as $l_t = \mathcal{D}(a_t)$. And the combination of all strokes in \mathcal{L} are constrained to compose M visually. In Ψ_v , the action sequence \mathcal{A} produced by the well trained DRL model is further converted to vector format \mathcal{V} in a designed manner.

The details of learning phase Ψ_l and vectorization phase Ψ_v are described in Section 3.2 and Section 3.3 respectively.

3.2. DRL Model Learning

In phase Ψ_l , our goal is to train a DRL model π to produce a suitable action sequence $\mathcal{A} = \{a_0, a_1, \dots, a_t\}$, and the action $a_t = \pi(s_t)$ is predicted by the observed state s_t in each timestep t . Each a_t can be converted to a stroke line $l_t = \mathcal{D}(a_t)$ by the drawing module \mathcal{D} , and all strokes can be combined into M visually. To improve the accuracy of each stroke, the stroke generation is designed to follow the *Markov Decision Process* and *Greedy Strategy*. In other words, the defined state space is independent of the timestep. In each timestep, according to the current state, the model only needs to find the next stroke line that is most suitable, and regardless of future strokes and final strokes combination.

Policy: as shown in Figure 2 left, our DRL model basically employs the model-based Deep Deterministic Pol-

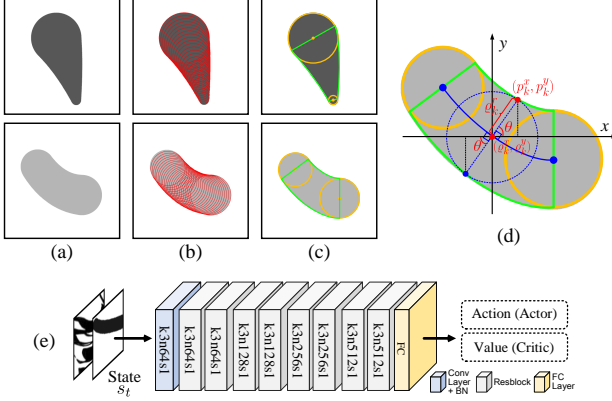


Figure 3: (a) Target stroke lines. (b) Stroke lines rendered by drawing module. (c) Vectorized stroke lines. (d) Details of stroke vectorization. (e) Network Architecture.

icy Gradient (DDPG) that follows the actor-critic architecture [13]. There are two networks, the actor $\pi(s_t)$ and critic $Q(s_t)$. The actor models a policy π that maps state s_t to action a_t , and the critic predicts the expected reward and is trained by

$$Q(s_t) = \mathcal{R}_t(a_t, s_t) + \gamma Q(s_{t+1}), \quad (1)$$

where $\mathcal{R}_t(a_t, s_t)$ is the current reward calculated by a_t and s_t , γ is the discount factor, and actor $\pi(s_t)$ is trained to maximize $Q(s_t)$.

State: our defined state s_t is independent from timestep t , and s_t consists of two parts: the current canvas c_t and the target manga M , represented as $s_t = (c_t, M)$. Initialize with a blank canvas c_0 , the actor π produces action $a_t = \pi(s_t)$ according to s_t , and $(t+1)$ -th canvas $c_{t+1} = c_t + \mathcal{D}(a_t)$ is rendered by the drawing module \mathcal{D} . Then, the next state s_{t+1} is represented as $s_{t+1} = [\mathcal{D}(\pi(s_t)), M]$.

Action and drawing module: the drawing module \mathcal{D} is designed to convert an action a_t to a stroke line l_t . Formally, $l_t = \mathcal{D}(a_t)$, $a_t \in [0, 1]$. Although training a neural render to map a_t to l_t is flexible (e.g., [13]), it will compromise strokes' accurateness (e.g., irregular or blurring edges, missing pixels) and the inaccuracy strokes are fatal to our task. Therefore, we design an image rendering program as the drawing module \mathcal{D} .

As shown in Fig. 3(a)(b), the path of a stroke line l_t follows the rules of quadratic Bézier curve (QBC) \mathcal{B} , and the thickness of l_t is controlled by a sequence of circles. Each circle ϱ_k is defined as $\varrho_k(\varrho_k^x, \varrho_k^y, \varrho_k^r)$, where ϱ_k^x , ϱ_k^y , and ϱ_k^r indicate x , y coordinates, and radius of ϱ_k respectively. Then, $\varrho_k(\varrho_k^x, \varrho_k^y, \varrho_k^r)$ is calculated by

$$\begin{aligned} \varrho_k^x &= (1 - k)^2 P_0^x + 2(1 - k)k P_1^x + k^2 P_2^x \\ \varrho_k^y &= (1 - k)^2 P_0^y + 2(1 - k)k P_1^y + k^2 P_2^y, \\ \varrho_k^r &= (1 - k)P_0^r + kP_2^r \end{aligned} \quad (2)$$

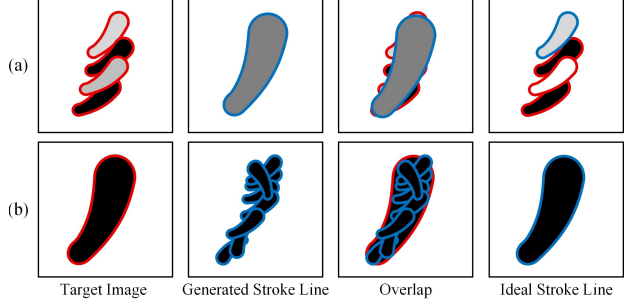


Figure 4: The original L2 reward makes the trained agent produce inaccurate strokes. (a) For dense strokes in the target image, the agent may cover multiple strokes with a larger stroke in an average color. (b) For a larger stroke in the target image, the agent may render the region with numerous smaller strokes repeatedly.

where P_0 , P_1 , and P_2 are the three control points of a QBC. Correspondingly, the designed action a_t consists of nine control parameters of a QBC, defined as

$$a_t = (P_0^x, P_0^y, P_1^x, P_1^y, P_2^x, P_2^y, P_0^r, P_2^r, g)_t, \quad (3)$$

where (P_0^x, P_0^y) , (P_1^x, P_1^y) , and (P_2^x, P_2^y) indicate the (x, y) coordinates of P_0 , P_1 , and P_2 respectively. (P_0^r, P_2^r) control a stroke's thickness, and g control a stroke's color in 1-channel grayscale space.

Reward: for designing the reward, our main goal is to select the most suitable and accurate stroke line l_t in each timestep t . The previous strokes generating work [13] presents that employing the L2 reward r_t can encourage the agent to gradually draw the target image, and the reward r_t is defined as

$$r_t = \|c_t - M\|^2 - \|c_{t+1} - M\|^2. \quad (4)$$

However, as shown in Figure 4, we observe in experiments that the original reward in Eq.(4) will make the trained model produce inaccurate strokes. On the one hand, for dense strokes in the target image, the actor will produce a larger stroke in the average color to cover a region with multiple strokes [Fig. 4(a)]. On the other hand, for a larger stroke in the target image, the agent will render the area by numerous smaller strokes repeatedly [Fig. 4(b)].

To produce stroke lines more accurately, we define $l_t = l_t^b \times g_t$, $c_{t+1} = c_t + l_t^b \times g_t$, where l_t^b and g_t indicate the coverage and the color of a stroke l_t respectively. l_t^b is a binary matrix consisting 1 and 0, and 1 (or 0) indicates a pixel is in (or not in) the stroke l_t . g_t is divided into 11 grayscale gradation, $g_t \in \mathcal{G}$, $\mathcal{G} = \{0, 0.1, 0.2, \dots, 1\}$. Then, we design

our SA (*Stroke Accurateness*) reward \mathcal{R}_t as:

$$\begin{aligned}
\mathcal{R}_t &= \lambda_1 r_1^t + \lambda_2 r_2^t + \lambda_3 r_3^t + \lambda_4 r_4^t \\
r_1^t(l_t) &= \frac{1}{CHW} \cdot \mathbf{Sum}(l_t^b) \\
r_2^t(l_t) &= 1 - \frac{1}{|\mathcal{G}|} \cdot \mathbf{Unique}(l_t^b \times M) \\
r_3^t(l_t, c_t, c_{t+1}) &= \frac{1}{CHW} \|l_t^b \times c_t - l_t^b \times c_{t+1}\|_2^2 \\
r_4^t(l_t, c_{t+1}, M) &= 1 - \frac{1}{CHW} \|l_t^b \times c_{t+1} - l_t^b \times M\|_2^2
\end{aligned} \tag{5}$$

where λ_1 to λ_3 are used to balance the multiple objectives. **Sum()** and **Unique()** are functions to calculate the sum and different elements number in parentheses. l_t , l_t^b , c_t , and c_{t+1} have the same shape of $C \times H \times W$, $\{r_1^t, r_2^t, r_3^t, r_4^t\} \in [0, 1]$. The meaning of r_1^t to r_4^t are as following:

- r_1^t is increasing with the coverage l_t^b of stroke.
- r_2^t is decreasing with the category number of colors in $(l_t^b \times M)$.
- r_3^t is increasing with the difference between $l_t^b \times c_t$ and $l_t^b \times c_{t+1}$.
- r_4^t is increasing with the similarity between $l_t^b \times c_t$ and $l_t^b \times M$.

Network Architecture: as shown in Figure 3(e), in order to produce accurate strokes to better handle mangas with complex textures, the actor and critic follow the network architectures of residual structures similar to ResNet-18 [12], and the critic uses WN [25] with Translated ReLU (TReLU) [31] to stabilize the learning. Referencing the method of model-based DDPG [13], we utilize the soft target network that constructs a copy for the actor and critic and updating their weights by making them slowly track the learned networks.

3.3. Vectorization

In the vectorization phase Ψ_v , as shown in Figure 2 right, utilizing the well trained actor π , Ψ_v can be modeled as $\Psi_v = \{\Phi_{m2a}, \Phi_{a2v}\}$. First, Φ_{m2a} generates a action sequence $\mathcal{A} = \{a_0, a_1, \dots, a_t\}$ following the content of manga M . Then, Φ_{a2v} translates action sequence \mathcal{A} to a vector graphic sequence $\mathcal{V} = \{v_0, v_1, \dots, v_t\}$. Formally, $\mathcal{V} = \Psi_v(M) = \Phi_{a2v}(\Phi_{m2a}(\pi, M))$.

Design of vectorized stroke: as shown in Figure 3(b), in drawing module \mathcal{D} , a stroke is rendered as hundreds of continuous circles (red) $\{\varrho_1, \varrho_2, \dots, \varrho_k\}$, where the path of circle centers follow a QBC \mathcal{B} as Eq.(2), and radiiuses of start and end circle are P_0^r and P_2^r defined in Eq.(2)(3). Although it is easy to vectorize a stroke by vectorizing each of these circles, the storage of the final vector graphic will be particularly large.

Algorithm 1: Pruning Algorithm.

```

Input:  $\mathcal{A}, M, \xi$ ;
1 Initialize  $t = |\mathcal{A}|$  ;
2  $\mathcal{V} \leftarrow \Phi_{a2v}(\mathcal{A})$  ;
3  $\delta \leftarrow \frac{\|M - I(\mathcal{V})\|_2^2}{CHW}$  ;
4 while  $t > 0$  do
5    $\mathcal{V}' \leftarrow \mathcal{V}$  ;
6   Remove  $v_t$  in  $\mathcal{V}'$  ;
7    $\delta' \leftarrow \frac{\|M - I(\mathcal{V}')\|_2^2}{CHW}$  ;
8   if  $\delta' \leq \delta + \xi$  then
9     |    $\delta \leftarrow \delta'$  ;
10    |    $\mathcal{V} \leftarrow \mathcal{V}'$  ;
11    |    $t \leftarrow t - 1$  ;
12   else
13     |    $t \leftarrow t - 1$  ;
14   end
15 end
Output:  $\mathcal{V}$ ;

```

To represent a vectorized stroke v_t in a light-weight manner, as shown in Figure 3(c), we define v_t as three parts, i.e., the start and end circles (yellow) and a enclosed path p (green). Since the widely used vector format (e.g., SVG, PDF) can only represent a curve as a QBC path, we must calculate the fitted QBC path of p 's edges.

As shown in Figure. 3(c)(d), first, we obtain ϱ_k 's radiiuses that are perpendicular to \mathcal{B} , and then find the intersection p_k of the radius and circle, calculated by

$$p_k^x = \varrho_k^x \pm \cos(\theta) \cdot \varrho_k^r, \quad p_k^y = \varrho_k^y \pm \sin(\theta) \cdot \varrho_k^r, \tag{6}$$

where (p_k^x, p_k^y) is the coordinate of p_k , $\theta = \arctan[(\mathcal{B}')^{-1}]$, and \mathcal{B}' indicates the derivative of \mathcal{B} , calculated by

$$\mathcal{B}' = \frac{d(\varrho_k^y)}{d(\varrho_k^x)} = \frac{(1-k)(P_1^y - P_0^y) + k(P_2^y - P_1^y)}{(1-k)(P_1^x - P_0^x) + k(P_2^x - P_1^x)}, \tag{7}$$

where P_0, P_1, P_2 are defined in Eq.(2)(3). The obtained p_k is a point on the curve edge of p , and we further calculate five points on each edge of p to fit a QBC paths.

Pruning Mechanism: in Φ_{m2a} , there are two points compromise the performance on vectorization. First, π may produces some error strokes to increase the difference between generated vector graph and the ground truth. Second, the strokes are stacked together where may have repeated or redundant strokes to increase the storages of vectorization results. To address these two issues, as shown in Algorithm 1, we propose a pruning mechanism to optimize the redundant strokes and the storage sizes.

In Algorithm 1, we input the action sequence \mathcal{A} and output the pruned vector sequence \mathcal{V} , where $|\mathcal{A}|$ indicate the cardinality of \mathcal{A} , M is the ground truth, $I(\mathcal{V})$ means converting \mathcal{V} to a raster image, and M and $I(\mathcal{V})$ have the same

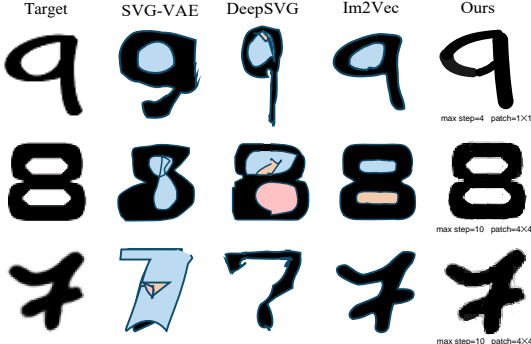


Figure 5: Vectorization on dataset FONTS with simple structure. The observed results demonstrate that compared with the leading learn-based vectorization methods, our Mang2Vec can produce accurate results for vectorizing raster images with simple structure (e.g., fonts).

size of $C \times H \times W$. v_t is the vectorized strokes produced by a_t , δ is the measured difference between $I(\mathcal{V})$ and M , and ξ indicates the tolerable error which is used to balance the visual similarity and the storage size of \mathcal{V} .

4. Experiment

In the following experiments, we mainly evaluate the performance of Mang2Vec on two aspects, the vectorization accurateness and the storage sizes of vectorization results.

4.1. Experimental Setting

Our Manga2Vec is implemented in PyTorch, and all experiments are performed on a computer with an NVIDIA Geforce RTX 2080 GPU. The dataset DeepManga used in experiments is collected from popular manga works and contains 42599 raster manga with 1024×1024 resolution. For training the DRL agent of Manga2Vec, each training data is converted to 1-channel grayscale space, and we randomly cut 128×128 images from original data as the inputs. The learning rate of actor or critic is $\{3 \times 10^{-4}, 1 \times 10^{-4}\}$ or $\{1 \times 10^{-3}, 3 \times 10^{-4}\}$, learning rate decays after 1×10^5 training batches, and the optimizer is Adam. We set 1 action per timestep, 40 timesteps per episode, and the reward discount factor is 0.95⁵. In all experiments, by default, we set $\delta_1, \delta_2, \delta_3, \delta_4 = 1$ in Eq.(5), the max numbers of strokes $\mathcal{S} = 40$, and the number of patches $\mathcal{P} = 32 \times 32$.

4.2. Vectorization Accurateness

Vectorization on simple structure: we first measure the vectorization performance of the related learn-based methods (including SVG-VAE [19], DeepSVG [3], and Im2Vec [23]) and ours on the dateset with simple structures (e.g., FONTS). As shown in Figure 5 and Table 1, the results are compared in subjective visual perception and objective in-

Table 1: Vectorization Accuracy

Index	MSE		SSIM	
	FONTS	DeepManga	FONTS	DeepManga
SVG-VAE	0.3815	×	0.4328	×
DeepSVG	0.3433	×	0.5238	×
Im2Vec	0.0532	0.2445	0.8083	0.3879
Ours	0.0261	0.0905	0.9303	0.7468

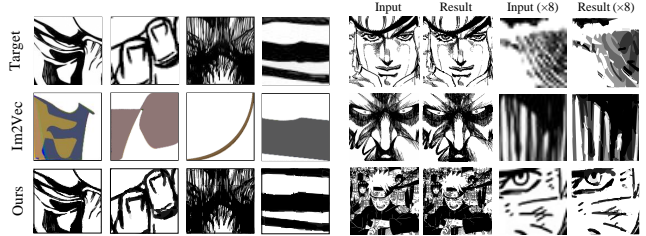


Figure 6: Vectorizations on mangas with complex structures. **Left:** comparison with the leading learning-based vectorization method Im2Vec trained by the same dataset DeepManga with us. **Right:** Our vectorization results in different zooming scales.

dexes of **MSE (Mean Square Error)** and **SSIM** [30] (*Structural SIMilarity*). MSE and SSIM are employed to measure the similarity between targets and outputs. MSE indexes are computed by $\frac{\|I - O\|^2}{CHW \times 255} \in [0, 1]$, where I and O indicate targets and outputs of sizes $C \times H \times W$, and $I, O \in [0, 255]$. SSIM indexes are in $[-1, 1]$, and the similarity between two images is proportional to the SSIM index. In comparing similarities, each method’s results in vector space are rasterized to 512×512 by CairoSVG [15].

Figure 5 and Table 1 demonstrate that compared with other learning-based methods, our method can produce vectorization results with high accuracy, and achieves the state-of-the-art level for vectorizing targets with simple structures.

Vectorization on complex structure: we also measure the vectorization performance on mangas with complex structures, and results are shown in Figure 6 and Table 1. We compare our method with the leading method Im2Vec [23] which trained by the same dataset DeepManga with us. Note that we do not compare with DeepSVG [3] and SVG-VAE [19], since they cannot be trained without the supervision of vector ground truth. Moreover, Reddy et al. [23] have proved that Im2Vec outperforms DeepSVG and SVG-VAE on the accurateness of vector reconstruction. Results in Figure 6 and Table 1 show that our method outperforms the referenced methods on the accurateness of vectorization mangas with complex structures.

Although the reference learn-based methods have the advantage of reproducing the intended vector parametrization,

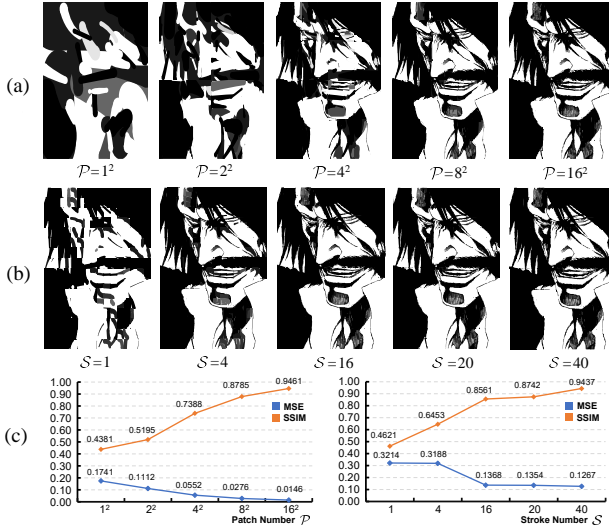


Figure 7: Our vectorization results in different numbers of patch \mathcal{P} and strokes \mathcal{S} . (a) Influence of \mathcal{P} , when $\mathcal{S} = 20$. (b) Influence of \mathcal{S} , when $\mathcal{P} = 16^2$. (c) Measurement of accurateness.

they can only handle targets with simple structures or textures (e.g., icons, fonts) due to the limitation of processable vector parameters. By contrast, our method is better at handling targets with complex textures since the strokes can be added infinitely by the DRL agent.

Influence of patches and strokes: in the vectorization phase, a result with higher accuracy can be produced by dividing the target image into small patches and vectorizing each of them respectively. In Figure 7, we display the vectorization results under the settings of different numbers of patches and strokes. The observed results show that vectorization accuracy is proportional to the number of patches and strokes. Moreover, after the stroke number reaches a threshold, the influence of stroke number increasing on the accuracy will be less and less.

Accuracy of strokes: for evaluating the accuracy of strokes, we mainly compare our performance with the baseline [13] of producing neural strokes. Comparisons in visual and quantification as shown in Figure 8, we observed that the stroke accuracy in positions and colors of our method is significantly higher than that of the baseline, and our method does better in the task of manga vectorization.

4.3. Storage Size and Time Cost

Storage size: in Mang2Vec, the pruning module (PM) is designed to reduce the storage size of vectorization results. Leveraging 100 random vectorization samples, we evaluate the performance of PM on two aspects, the reduced storage size and the influence of size reduction on visual similarity. As shown in Figure 9 upper, using PM is able to

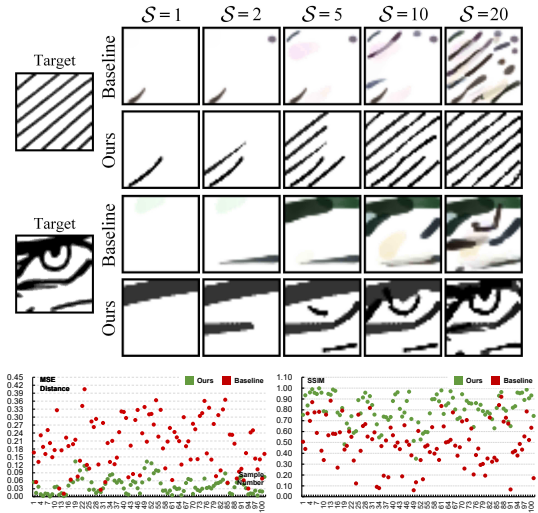


Figure 8: Compared with the baseline [13] of producing neural strokes. **Upper:** Visual comparisons in different stroke numbers \mathcal{S} . **Bottom:** Quantitative differences between targets and outputs in 100 random samples when $\mathcal{S}=40$. The left and right scatter charts show the results measured by methods of MSE and SSIM respectively.

reduce about 50% of the storage sizes when $\mathcal{S} = 40$, and the effectiveness is proportional to the maximum numbers of strokes. In Figure 9 bottom, we display the visual similarity between target and vectorization results. The scatter charts show that the reduction of storage size preserves or even improves the visual similarity since PM removes the redundant and error stroke lines.

To summarize, PM effectively reduces the storage sizes of outputs without compromising the visual similarity of vectorization.

Time cost: we evaluate the time cost of Mang2Vec on vectorization without PM and the time cost of PM. Let \mathcal{P} and \mathcal{S} indicate the patch number patch and the stroke number respectively, and the calculated time costs (in seconds) are shown in Table 2. The results demonstrate that the time costs of our method are increasing with \mathcal{P} and \mathcal{S} , and the maximum vectorization time is an acceptable few minutes. Empirically, setting $\mathcal{P} = 16$, $\mathcal{S} = 20$ is enough to produce results in high accuracy, and setting $\mathcal{P} = 32$, $\mathcal{S} = 40$ can already handle mangas with extremely complex structures.

5. Advantage and Limitation

According to the advantages of images vectorization aforementioned in Section I, our vectorized mangas are resolution-independent and readily displayed on digital devices with different resolutions, and have smaller storage sizes than raster images when representing some target contents.

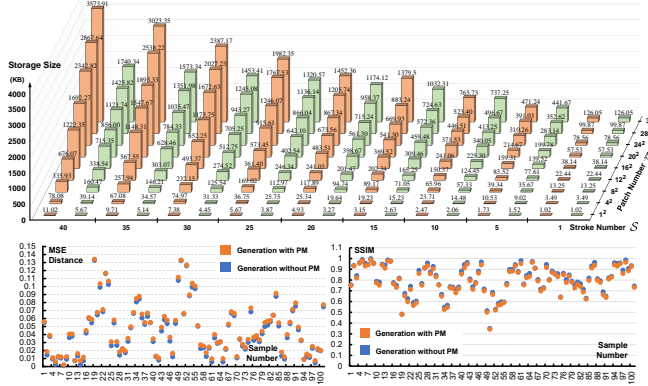


Figure 9: Influences of using pruning module (PM) on storage size and visual similarity. **Upper:** average storage sizes (kilobyte) of vectorized results (in 100 random samples) generating without PM (red) and with PM (green). **Bottom:** Quantitative similarity between targets and outputs in 100 random cases. The results show that PM effectively reduces the storage sizes of outputs without compromising the visual similarity.

Table 2: Time costs (seconds) under different numbers of patch \mathcal{P} and stroke \mathcal{S} . **Upper:** time costs of Mang2Vec w/o pruning module. **Bottom:** time costs of the pruning module.

$\mathcal{P} \setminus \mathcal{S}$	1	5	10	15	20	25	30	35	40
1^2	1.22	1.28	1.31	1.35	1.39	1.45	1.50	1.54	1.58
4^2	1.37	1.74	2.22	2.70	3.19	3.67	4.06	4.51	4.97
8^2	1.72	3.43	5.18	7.18	8.91	10.72	12.54	14.35	16.96
12^2	2.45	6.59	12.36	16.32	21.84	26.34	29.12	34.12	37.43
16^2	3.34	10.11	18.15	23.62	33.68	39.24	49.46	53.24	68.60
20^2	4.65	13.25	27.46	37.58	52.63	63.24	76.67	83.14	92.32
24^2	5.92	21.62	39.65	55.28	75.68	91.35	109.43	113.43	118.53
28^2	7.46	28.12	52.38	83.03	102.71	134.62	150.87	189.41	201.99
32^2	9.36	35.89	69.81	98.60	116.35	148.35	185.65	225.32	257.34
$\mathcal{P} \setminus \mathcal{S}$	1	5	10	15	20	25	30	35	40
1^2	0.02	0.08	0.18	0.22	0.47	0.8	1.08	1.22	2.33
4^2	0.18	0.61	1.54	2.75	5.18	7.82	12.76	18.12	26.53
8^2	0.58	2.11	5.32	10.98	18.95	32.34	49.56	71.31	97.61
12^2	1.53	7.18	12.34	22.98	34.17	50.37	69.25	95.34	189.18
16^2	2.94	11.75	20.48	31.63	48.23	93.24	123.85	165.76	323.71
20^2	4.94	20.13	33.53	64.55	101.34	143.71	198.35	256.37	358.35
24^2	8.31	28.74	46.08	92.96	144.79	203.84	283.63	372.54	517.37
28^2	12.83	34.97	69.77	125.74	197.36	279.56	387.19	503.87	697.64
32^2	20.23	51.54	98.14	165.25	257.23	367.95	506.45	658.32	921.61

However, our Mang2Vec is a primitive-based method that is a new view to produce a vector graphic consisting of numerous vector primitives. This is much different from other methods that mainly produce some key vector paths (e.g., [3, 19, 23]). Therefore, Mang2Vec has slight limitations in aspects of shape retrieval and content edits.

6. Conclusion

In this paper, we propose Mang2Vec, the first approach for vectorizing raster mangas based on Deep Reinforcement Learning. We present a new view that regards an entire manga as a collection of primitives "stroke line", and the sequence of strokes lines can be deep decomposed for vectorization. To improve our performance on vectorization accuracy and storage size, we further propose an SA reward and a pruning mechanism in Mang2Vec. Quantitative and qualitative experiments demonstrate that our Mang2Vec can produce impressive results and reaches the state-of-the-art level.

References

- [1] Samaneh Azadi, Matthew Fisher, Vladimir G Kim, Zhaowen Wang, Eli Shechtman, and Trevor Darrell. Multi-content gan for few-shot font style transfer. In *Proceedings of the IEEE conference on computer vision and pattern recognition*, pages 7564–7573, 2018. 2
- [2] Mikhail Bessmeltsev and Justin Solomon. Vectorization of line drawings via polyvector fields. *ACM Transactions on Graphics (TOG)*, 38(1):1–12, 2019. 2
- [3] Alexandre Carlier, Martin Danelljan, Alexandre Alahi, and Radu Timofte. Deepsvg: A hierarchical generative network for vector graphics animation. *arXiv preprint arXiv:2007.11301*, 2020. 2, 6, 8
- [4] Edoardo Alberto Dominici, Nico Schertler, Jonathan Griffin, Shayan Hoshyari, Leonid Sigal, and Alla Sheffer. Polyfit: perception-aligned vectorization of raster clip-art via intermediate polygonal fitting. *ACM Transactions on Graphics (TOG)*, 39(4):77–1, 2020. 2
- [5] Luca Donati, Simone Cesano, and Andrea Prati. An accurate system for fashion hand-drawn sketches vectorization. In *Proceedings of the IEEE International Conference on Computer Vision (ICCV) Workshops*, Oct 2017. 2
- [6] Vage Egiazarian, Oleg Voynov, Alexey Artemov, Denis Volkonskiy, Aleksandr Safin, Maria Taktasheva, Denis Zorin, and Evgeny Burnaev. Deep vectorization of technical drawings. In *European Conference on Computer Vision*, pages 582–598. Springer, 2020. 2
- [7] Jean-Dominique Favreau, Florent Lafarge, and Adrien Bousseau. Fidelity vs. simplicity: a global approach to line drawing vectorization. *ACM Transactions on Graphics (TOG)*, 35(4):1–10, 2016. 3
- [8] Jun Gao, Chengcheng Tang, Vignesh Ganapathi-Subramanian, Jiahui Huang, Hao Su, and Leonidas J Guibas. Deepspline: Data-driven reconstruction of parametric curves and surfaces. *arXiv preprint arXiv:1901.03781*, 2019. 2
- [9] Yue Gao, Yuan Guo, Zhouhui Lian, Yingmin Tang, and Jianguo Xiao. Artistic glyph image synthesis via one-stage few-shot learning. *ACM Transactions on Graphics (TOG)*, 38(6):1–12, 2019. 2
- [10] Yi Guo, Zhuming Zhang, Chu Han, Wenbo Hu, Chengze Li, and Tien-Tsin Wong. Deep line drawing vectorization via

line subdivision and topology reconstruction. In *Computer Graphics Forum*, volume 38, pages 81–90. Wiley Online Library, 2019. 2

[11] David Ha and Douglas Eck. A neural representation of sketch drawings. *arXiv preprint arXiv:1704.03477*, 2017. 2

[12] Kaiming He, Xiangyu Zhang, Shaoqing Ren, and Jian Sun. Deep residual learning for image recognition. In *Proceedings of the IEEE conference on computer vision and pattern recognition*, pages 770–778, 2016. 5

[13] Zhewei Huang, Wen Heng, and Shuchang Zhou. Learning to paint with model-based deep reinforcement learning. In *Proceedings of the IEEE/CVF International Conference on Computer Vision*, pages 8709–8718, 2019. 3, 4, 5, 7

[14] Johannes Kopf and Dani Lischinski. Depixelizing pixel art. In *ACM SIGGRAPH 2011 papers*, pages 1–8. 2011. 2

[15] Kozea. Cairosvg. <https://cairosvg.org/>. 6

[16] Gregory Lecot and Bruno Levy. Ardeco: Automatic region detection and conversion. In *17th Eurographics Symposium on Rendering-EGSR’06*, pages 349–360, 2006. 2

[17] Tzu-Mao Li, Michal Lukáč, Michaël Gharbi, and Jonathan Ragan-Kelley. Differentiable vector graphics rasterization for editing and learning. *ACM Transactions on Graphics (TOG)*, 39(6):1–15, 2020. 3

[18] Chen Liu, Jiajun Wu, Pushmeet Kohli, and Yasutaka Furukawa. Raster-to-vector: Revisiting floorplan transformation. In *Proceedings of the IEEE International Conference on Computer Vision (ICCV)*, Oct 2017. 2

[19] Raphael Gontijo Lopes, David Ha, Douglas Eck, and Jonathon Shlens. A learned representation for scalable vector graphics. In *Proceedings of the IEEE/CVF International Conference on Computer Vision*, pages 7930–7939, 2019. 2, 6, 8

[20] Reiichiro Nakano. Neural painters: A learned differentiable constraint for generating brushstroke paintings. *arXiv preprint arXiv:1904.08410*, 2019. 3

[21] Giacchino Noris, Alexander Hornung, Robert W Sumner, Maryann Simmons, and Markus Gross. Topology-driven vectorization of clean line drawings. *ACM Transactions on Graphics (TOG)*, 32(1):1–11, 2013. 2

[22] Alexandrina Orzan, Adrien Bousseau, Holger Winnemöller, Pascal Barla, Joëlle Thollot, and David Salesin. Diffusion curves: a vector representation for smooth-shaded images. *ACM Transactions on Graphics (TOG)*, 27(3):1–8, 2008. 2

[23] Pradyumna Reddy, Michael Gharbi, Michal Lukac, and Niloy J Mitra. Im2vec: Synthesizing vector graphics without vector supervision. In *Proceedings of the IEEE/CVF Conference on Computer Vision and Pattern Recognition*, pages 7342–7351, 2021. 2, 6, 8

[24] Leo Sampaio Ferraz Ribeiro, Tu Bui, John Collomosse, and Moacir Ponti. Sketchformer: Transformer-based representation for sketched structure. In *Proceedings of the IEEE/CVF Conference on Computer Vision and Pattern Recognition*, pages 14153–14162, 2020. 2

[25] Tim Salimans and Durk P Kingma. Weight normalization: A simple reparameterization to accelerate training of deep neural networks. *Advances in neural information processing systems*, 29:901–909, 2016. 5

[26] Gopal Sharma, Rishabh Goyal, Difan Liu, Evangelos Kalogerakis, and Subhransu Maji. Neural shape parsers for constructive solid geometry. *IEEE Transactions on Pattern Analysis and Machine Intelligence*, 2020. 3

[27] Ayan Sinha, Asim Unmesh, Qixing Huang, and Karthik Ramani. Surfnet: Generating 3d shape surfaces using deep residual networks. In *Proceedings of the IEEE conference on computer vision and pattern recognition*, pages 6040–6049, 2017. 2

[28] Hao Su, Jianwei Niu, Xuefeng Liu, Qingfeng Li, Jiahe Cui, and Ji Wan. Mangagan: Unpaired photo-to-manga translation based on the methodology of manga drawing. In *Proceedings of the AAAI Conference on Artificial Intelligence*, volume 35, pages 2611–2619, 2021. 2

[29] Hao Su, Jianwei Niu, Xuefeng Liu, Qingfeng Li, Ji Wan, Mingliang Xu, and Tao Ren. Artcoder: An end-to-end method for generating scanning-robust stylized qr codes. In *Proceedings of the IEEE/CVF Conference on Computer Vision and Pattern Recognition*, pages 2277–2286, 2021. 2

[30] Zhou Wang, Alan C Bovik, Hamid R Sheikh, and Eero P Simoncelli. Image quality assessment: from error visibility to structural similarity. *IEEE transactions on image processing*, 13(4):600–612, 2004. 6

[31] Song-Hai Zhang, Tao Chen, Yi-Fei Zhang, Shi-Min Hu, and Ralph R Martin. Vectorizing cartoon animations. *IEEE Transactions on Visualization and Computer Graphics*, 15(4):618–629, 2009. 2

[32] Ningyuan Zheng, Yifan Jiang, and Dingjiang Huang. Strokenet: A neural painting environment. In *International Conference on Learning Representations*, 2018. 3